MECHANISMS CONTROLLING THE AIR-SEA FLUX OF CO_2 IN THE NORTH ATLANTIC

MICK FOLLOWS
Program in Atmospheres, Oceans and Climate
Department of Earth Atmosphere and Planetary Sciences
Massachusetts Institute of Technology, Cambridge, MA, USA
mick@ocean.mit.edu

RICHARD G. WILLIAMS
Oceanography Laboratories
Department of Earth and Ocean Sciences
University of Liverpool, Liverpool, England
ric@liv.ac.uk

INTRODUCTION

The air-sea flux of carbon is controlled by the disequilibrium in partial pressure of carbon dioxide between the atmosphere and surface ocean. This disequilibrium is a consequence of the interactions of physical, chemical and biological processes in the ocean and, today, includes a response to the anthropogenic increase of atmospheric pCO_2. Fig. 1 illustrates the annual mean air-sea flux of carbon, $\mathcal{F}$, estimated from a knowledge of the atmospheric partial pressure, pCO_2^{at}, and compilation of surface pCO_2 observations by Takahashi *et al.* (1999). The air-sea flux of carbon is determined by

$$\mathcal{F} = -K_g K_0 (pCO_2 - pCO_2^{at}), \tag{1}$$

where K_0 is the solubility of CO_2 at local temperature and salinity. K_g is the air-sea gas transfer coefficient, which is dependent on local environmental conditions and is usually parameterized as a function of wind speed, sea-surface temperature and sea-surface salinity (Wanninkhof, 1992). The major global scale features in Fig. 1 are the outgassing of CO_2 from the tropical oceans, and the influx at mid and high latitudes. In this chapter we focus on understanding what sets the basin wide, and regional patterns of air-sea carbon flux in the North Atlantic basin. While we focus on the North Atlantic, some of the concepts and discussions are also relevent to other regions of the ocean.

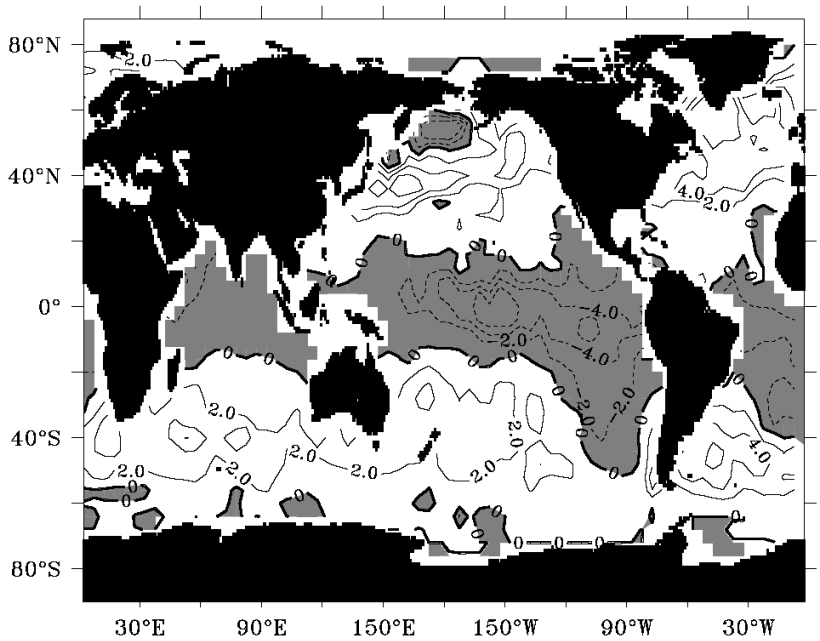

Figure 1. Air-sea flux of carbon, $mol\ m^{-2}\ yr^{-1}$ estimated from a global compilation of surface pCO_2 observations by Takahashi *et al.* (1999). Shaded areas indicate outgassing. The map is derived from a compilation of pCO_2 observations made over a number of years and the pattern has been normalized to the situation in 1990. However, the map still reflects a transient situation due to fossil fuel burning and the rapid increase in pCO_2^{at} in the past century (Takahashi *et al.*, 1999).

In Section 1, we briefly describe the distribution of carbon in the Atlantic basin and its relation to other water-mass properties. Then, in Section 2, we discuss how the large scale overturning circulation helps to drive a net basin flux of carbon into the ocean over the basin. We discuss the connections between the sub basin-scale patterns of the air-sea carbon flux, heat flux, and biological production in Section 3 and formalize these relationships in Section 4, where we describe the surface ocean carbon system following a water parcel moving through the surface Atlantic Ocean. In Section 5, we illustrate how the long timescale for equilibration of mixed-layer carbon with the atmosphere impacts the air-sea flux patterns using a numerical model. We discuss the role of the subduction process and the importance of the reservoir of carbon within the ventilated thermocline in Section 6. In Section 7, we speculate on the importance of time-varying, eddy circulations for the air-sea flux of carbon and, in Section 8, we briefly discuss the role of interannual variations.

1. THE DISTRIBUTION OF DISSOLVED INORGANIC CARBON IN THE ATLANTIC

There is a general increase in the concentration of dissolved inorganic carbon (DIC) with depth in the oceans (Fig. 2a). This storage in the thermocline and deep waters, away from the surface ocean and atmosphere, is achieved through a combination of physical and biological processes, referred to as 'pumps'. The total amount of dissolved carbon in a water parcel is enhanced due to the chemistry of the carbonate system in seawater (Murray, this volume). At equilibrium with a fixed atmospheric partial pressure, cooler waters can hold more dissolved inorganic carbon, DIC, than warm waters. Hence there is some increase in DIC with depth because cool, dense high latitude surface waters form the deep waters of the ocean (Fig. 2b). This effect is referred to as the *solubility pump* (Volk and Hoffert, 1985).

While the DIC distribution does reflect the undulations of the thermocline, marked by the enhanced vertical gradient in T over the upper 1 km, there are very large-scale interleaving patterns of DIC in the deep waters which are not prominent in T. However, similar patterns are revealed in salinity, S (Fig. 2c); a conservative tracer away from the surface of the ocean. For example, salty North Atlantic deep water spreads southwards from the deep water formation regions in the Labrador and Greenland seas at depths between 1000 and 3000 m. Fresher water spreads northwards at intermediate depths, as Antarctic Intermediate Water (around 1000 m), and as Antarctic Bottom Water along the seafloor. The thicker subtropical thermoclines are also highlighted by their saline character, due to strong net evaporation from the warm surface waters. These features are echoed by the DIC distribution.

This general correspondence between the distributions of DIC and S in the deep waters reflects transport of water masses from their point of subduction (see Section 6) and ventilation through the global oceans. In contrast to salinity, however, there is an interior source of DIC leading to enhanced vertical, and basin to basin, gradients. This interior source is due to biological processes and is termed the *biological pump*. In the process of photosynthesis, phytoplankton convert dissolved inorganic carbon and nutrients (such as nitrate, phosphate and iron) into organic matter (Anderson and Totterdell, this volume). This conversion occurs in the euphotic zone, typically the upper 100 m or so of the ocean where there is sufficient solar radiation. While the organic matter is cycled and transformed within the pelagic ecosystem, ultimately a fraction either sinks to depth as detritus or fecal matter, or is transported downwards in dissolved organic form (Hansell and Carlson, 1999). The exported organic matter is remineralized to inorganic form at depth, thus increasing the vertical contrast in DIC. This transfer is the *soft tissue pump*. There is an additional contribution from the calcium carbonate structural material formed

by certain planktonic species termed the *carbonate pump* (Volk and Hoffert, 1985).

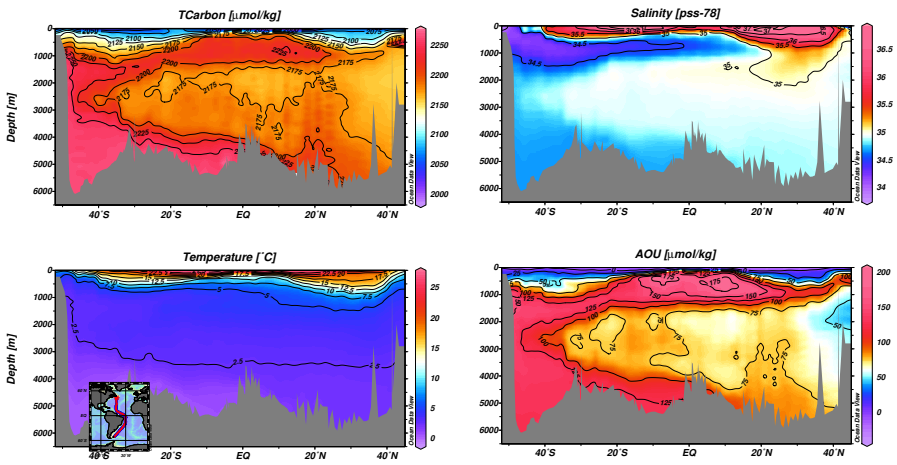

Figure 2. Atlantic meridional distributions of **(a)** dissolved inorganic carbon ($\mu mol\ kg^{-1}$), **(b)** temperature (^oC), **(c)** salinity (psu), and **(d)** apparent oxygen utilization ($\mu mol\ kg^{-1}$). Data are from the WOCE-JGOFS (World Ocean Circulation Experiment-Joint Global Ocean Flux Study) global survey. (Plotted using Ocean Data View.)

The remineralization of organic matter is accompanied by a consumption of oxygen. The stoichiometry of this conversion is reasonably well defined and dissolved oxygen is generally close to saturation in the surface waters. Hence the amount of organic matter which has been remineralized in a water parcel can be inferred from the "apparent oxygen utilization", defined $AOU = [O_2]_{sat}(T,S) - [O_2]$. Here $[O_2]$ is the *in situ* concentration of dissolved oxygen and $[O_2]_{sat}(T,S)$ is the saturated concentration, the concentration the water parcel is assumed to have had at the time it left the surface waters and inferred from its T and S. AOU has a strong maximum between 200 and 2000 m (Fig. 2d), the layer where most of the sinking organic matter is remineralized. AOU is also high in the older, deeper waters of the ocean due to the long term accumulation of remineralized carbon. The DIC and AOU distributions in Figs. 2a and d show a strong similarity due to the significant influence of the soft tissue pump on the DIC distribution.

In brief, the ocean DIC distribution has strong relationships with temperature, conservative water mass tracers like salinity, and indicators of biological processes such as AOU. It is clear that the solubility and biological pumps both are significant in setting the carbon distribution in the ocean. Both pumps are intimately linked with water masses and transport by the large-scale ocean circulation.

2. THE NET AIR-SEA FLUX OF CARBON OVER THE NORTH ATLANTIC

In the annual mean there is a net air-to-sea flux of carbon over most of the North Atlantic, with a small region of net outflux in the tropics, as depicted in (Fig. 1). Takahashi *et al.* (1999) estimated a net, basin wide air-sea flux of CO_2 (normalized to 1990) of about 0.7 $GtCy^{-1}$ into the Atlantic Ocean north of the Equator. The surface waters do not generally reach equilibrium with the overlying atmosphere, $pCO_2 \neq pCO_2^{at}$, due to the oceanic transport of DIC and the continual experience of thermal and biological forcing, including the seasonal cycle (e.g. Brostrom, 2000).

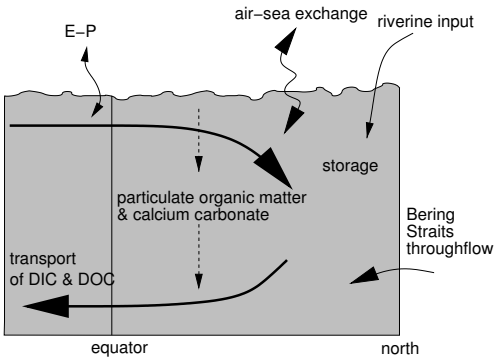

Figure 3. Schematic figure indicating the processes and fluxes which control the carbon distribution and net air-sea flux in the North Atlantic basin. Consider the box in the schematic to represent the North Atlantic basin from equator to its Northern extent. There is a net flux of carbon across the sea surface which is balanced by a combination of local storage, large scale transport of DIC and other processes, including riverine inputs, flow through the Bering Straits and transport of dissolved organic carbon, DOC.

The basin scale uptake of carbon is tied to the thermal and freshwater forcing of the region. Warm, low solubility surface waters are transported Northwards in the Atlantic and cooled, inducing the oceanic uptake of carbon, reinforced by biological transfer carbon and nutrients to the deep ocean. The contrast in thermal and freshwater forcing over the basin also supports the overturning circulation so the cold, carbon-rich deep water is transported southwards out of the North Atlantic (Fig. 3). Hence there is a net transport of carbon to the south at low latitudes. Holfort *et al.* (1998) estimated the net southwards transport of carbon at 20°S to be $2150 \pm 200 kmol\ s^{-1}$ (or about 0.8 $Gt\ C\ yr^{-1}$) from several observed transects of hydrography and DIC between 11°S and 30°S. Fig. 4 illustrates the depth dependence of the carbon transport (at 30°S) which, since the vertical change in DIC is small relative to the ocean mean value,

closely follows the structure of the mass flux associated with the overturning circulation. The estimate of net southward transport is of comparable magnitude to the basin wide air-sea flux estimated by Takahashi *et al.* (1999). However Lundberg and Haugan (1996) estimate a flux of carbon into the Atlantic from the Bering Straits and through the Arctic ocean also of similar magnitude, about $0.8\ Gt\ C\ yr^{-1}$, associated with a net volume flux of about $1Sv$. Hence the flow out of the North Atlantic to the south seems to be roughly balanced by flow in from the north and other processes must be invoked to balance the air-sea exchange in the budget including the accumulation of carbon within the basin, the effect of net surface freshwater fluxes, and riverine inputs of carbon and freshwater.

In addition, the transport and transformations of particulate and dissolved organic carbon (POC and DOC respectively) may be significant but are not yet quantified. Surface DOC concentration varies seasonally, between 40 and 60 $\mu mol\ kg^{-1}$ near Bermuda (Hansell and Carlson, 1999). At depth, it is relatively uniform at about 40 $\mu mol\ kg^{-1}$. The opposing vertical gradient suggests a DOC transport associated with the overturning circulation which may oppose that of DIC. The regional impact of DOC transport is, however, yet to be quantified.

The observed air-sea flux (Fig. 1) includes a contribution due to the air-sea disequilibrium caused by fossil fuel burning, on top of the pre-industrial pattern. The signature of the anthropogenic perturbation on oceanic DIC has been estimated (Gruber, 1998; Sabine et al. 1999). The role of the North Atlantic in responding to the atmospheric increase is currently unclear. As the North Atlantic is generally a sink of carbon from the atmosphere we might expect that is absorbs anthropogenic carbon accordingly. However, inversions of transport estimates (Wallace, 2001) and direct flux determinations (Lefevre et al., 2003) suggest that there might be a local loss of anthropogenic carbon from ocean to atmosphere. This unexpected inference could be due to a horizontal supply of anthropogenic carbon, absorbed elsewhere in the global ocean, and transported into the North Atlantic. Sarmiento *et al.* (2003) illustrate the importance of Southern Ocean mode waters as a source of nutrients to the North Atlantic basin: transport in this water mass might also be significant for the anthropogenic carbon budget.

In summary, while there is uncertainty in terms of the anthropogenic carbon budget and the cycling of DOC, the climatological picture of the basin-scale uptake of CO_2 from the atmosphere is broadly in accord with what is expected from the surface thermal and biological forcing and the DIC transport by the overturning circulation. In the following sections we discuss what sets the regional, sub-basin scale patterns of the air-sea flux (as shown in Fig. 5a) which reflect the impact of the gyre-scale circulation.

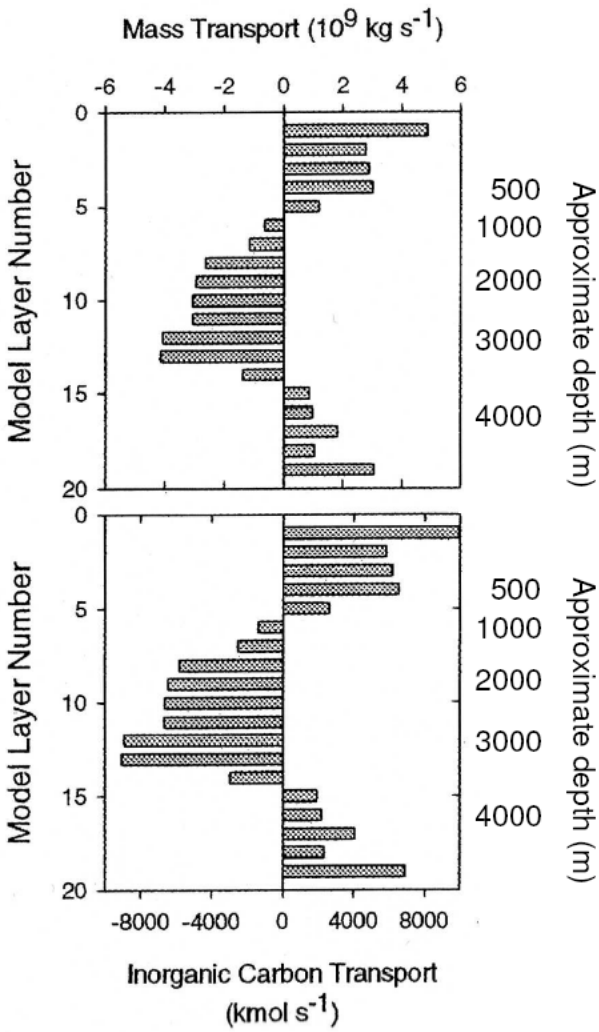

Figure 4. Zonally-integrated fluxes of mass and dissolved inorganic carbon (upper and lower panels) as a function of depth at 30°S in the Atlantic basin from Holfort *et al.* (1998). Note how the mass and carbon transports have a similar vertical structure with a northwards flux of surface and bottom waters, and a southwards flux of North Atlantic Deep Water. Figure adapted from Holfort *et al.* (1998).

3. REGIONAL PATTERN OF THE AIR-SEA CARBON FLUX

The regional variation of the air-sea flux of CO_2 in the North Atlantic basin is shown in Fig. 5a from the estimate of Takahashi *et al.* (1999) - a detail of Fig. 1. As noted earlier, there is an uptake of CO_2 by the oceans over almost all of the basin northwards of 10°N with outgassing in the tropics. This

pattern reflects the interaction of solubility effects, biological processes and the gyre scale circulation of the North Atlantic. Here we discuss these sometimes competing influences.

3.1 AIR-SEA HEAT FLUX AND SOLUBILITY FORCING

The regional pattern of the air-sea flux of CO_2 partly reflects that of the air-sea heat flux in which an uptake of CO_2 corresponds with a surface cooling, compare Fig. 5a and b (the latter as compiled by Josey *et al.*, 1998). The equilibrium surface ocean concentration of DIC, for a given atmospheric pCO_2 varies linearly with sea surface temperature. Hence the air-sea flux of heat drives changes in the surface equilibrium DIC concentration. The two maps reveal strong ocean uptake of CO_2 (unshaded) in the regions of strong oceanic heat loss (unshaded) over the Gulf Stream system and the subpolar gyre. On the integrated basin scale, this connection has been exploited by Watson *et al.* (1995) to estimate the air-sea CO_2 flux from the observed basin scale heat transport (together with estimates of nutrient and alkalinity changes accounting for the biological contributions).

However, the North Atlantic air-sea flux of CO_2 differs in detail from the pattern of the surface heat flux. For example, over the subtropical ocean, there is an oceanic uptake of CO_2, even in regions of a weak surface heat uptake (which is acting to decrease the solubility).

So why does the subtropical gyre of the North Atlantic absorb CO_2 since it is not a direct response to local heat forcing? We will discuss several possible explanations: Biological drawdown, the increase of atmospheric CO_2, and the role of physical transport of carbon in the ocean.

3.2 BIOLOGICAL DRAWDOWN OF CO_2

The distribution of chlorophyll-a in the surface North Atlantic is shown in Fig. 5c, revealing vigorous biological production at high latitudes and close to the eastern boundary. Much of the associated primary production (a measure of the rate of formation of organic matter by photosynthesis) is associated with locally recycled carbon and nutrients. A small fraction however, termed export production, is transferred into the deep ocean through a combination of sinking of organic particles and advection of dissolved organic matter. Export production reduces the surface DIC concentration and is expected to lead to an uptake of CO_2 over the whole basin. This contribution reinforces the local cooling and increase in solubility at higher latitudes and may be significant in the tropics and coastal waters, where it opposes the local tendency in solubility due to local warming. Due to variations in the rate of local recycling, export production is probably less variable across the basin relative to primary pro-

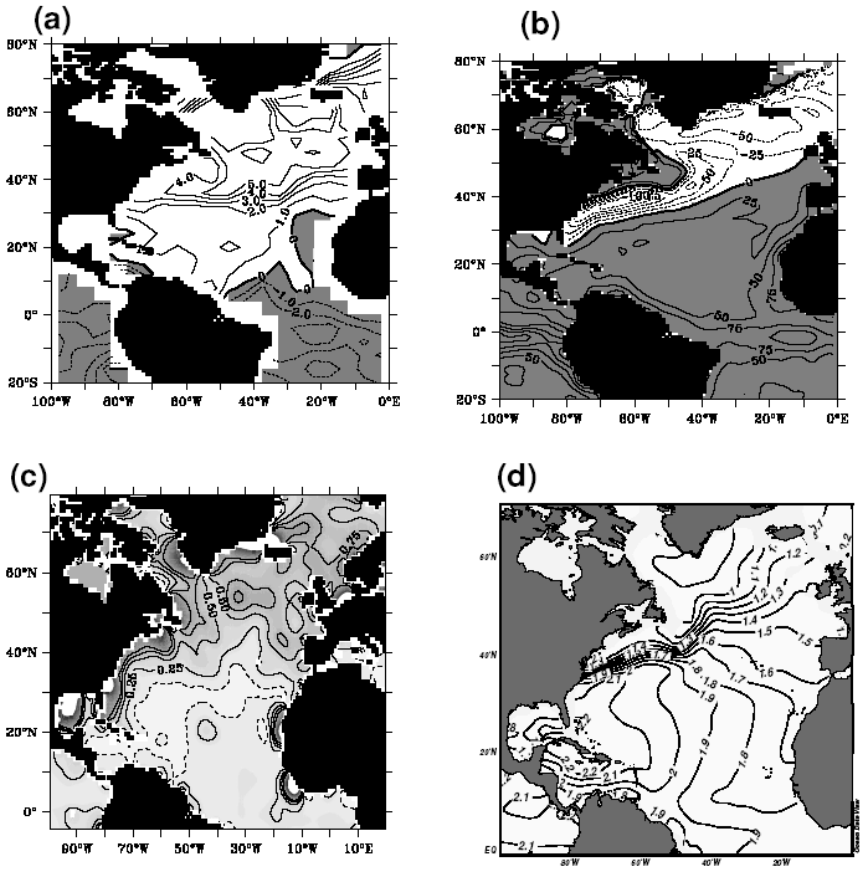

Figure 5. (a) Air-sea flux of CO_2, $mol\ m^{-1}\ yr^{-1}$ (Data from Takahashi *et al., 1999*). Shaded regions correspond to a loss of CO_2 to the atmosphere. (b) Annual mean air-sea flux of heat, Wm^{-2}, in the North Atlantic (Data from Josey *et al.*, 1998). Negative values (unshaded) denote a loss of heat to the atmosphere and a corresponding increase in solubility of CO_2. The difference in the extent of the shaded regions between (a) and (b) indicates the regions where carbon and heat flux are decoupled. (c) Climatological surface ocean chlorophyll-a concentration ($\mu g\ l^{-1}$) from the World Ocean Atlas (Conkright *et al.*, 2001). The chlorophyll distribution suggests vigorous biological productivity and the strong spring bloom in the subpolar regions, and the nutrient limited subtropical gyre, broadly corresponding to the patterns of gyre-scale upwelling and downwelling. (d) Dynamic height relative to 2000m (dyn m) in the North Atlantic, derived from the climatological hydrography of the WOA01 atlas (Conkright et al., 2002). Upper ocean geostrophic circulation approximately follows the contours and is inversely proportional to the distance between them. The figure reveals the anti-cyclonic flow of the subtropical gyre, the swift flow close to the western boundary (tight contours) and the cyclonic subpolar circulation.

duction (Emerson et al., 1997). In the subtropics the rate of export production is ultimately limited by the slow rate of nutrient supply to the surface. In addition, nutrients transported from the deep ocean to the surface may bring with

them excess carbon of biogenic origin, sufficient to provide the necessary carbon for organic matter without requiring a flux across the sea surface (Lewis 1992). This transfer of biogenic carbon is tied up with the concept of fixed stoichiometry for biological transformations and the Redfield ratio (see Anderson and Totterdell, 2003, this volume) and we discuss this further in the next section.

3.3 ATMOSPHERIC TRANSIENT OF CO_2

Over the past century atmospheric pCO_2 has been increasing due to fossil fuel emissions at a (variable) rate of about 1 $ppmv\ yr^{-1}$. To what extent is the uptake of CO_2 by the subtropical gyres due to the rapid increase in atmospheric pCO_2^{at}? While this factor might increase the air-sea flux in those regions, numerical models consistently suggest there would have been a flux of CO_2 into the pre-industrial subtropical gyres. For example, the preindustrial simulations in all of the OCMIP (Ocean Carbon-cycle Model Intercomparison Project) models summarized by Orr (2002).

3.4 DELAYED RESPONSE OF CO_2 FLUX

In our view there is another important factor driving the uptake of CO_2 over the subtropical gyres; the long equilibration timescale for mixed layer carbon which causes the air-sea flux response to take place downstream of the regions of strong solubility and biological forcing.

The upper ocean circulation of the North Atlantic can be inferred (Fig.5d) from the dynamic height of the water column relative to 2000m. The figure reveals the anti-cyclonic, subtropical gyre and the intense western boundary current including tight, inertial recirculations. Part of the fluid in the western boundary recirculates around the subtropical gyre, while the rest is swept further north into the cyclonic, subpolar gyre, where it is cooled and converted to a denser water mass. With respect to the subtropical gyre, the regions of most intense solublility and biological forcing are associated with the region of the Gulf Stream, with intense cooling, and the gyre margins, where there is significant biological drawdown. The anomalies generated by these processes in the margins are transported into the interior of the gyre in the anti-cyclonic gyre flow where they are gradually eroded by the air-sea flux.

The significance of this delayed response is supported by numerical models which have a lagged response to cooling over the Gulf Stream (Sarmiento *et al.*, 1995) which extends downstream into the interior of the subtropical gyre (Follows *et al.*, 1996; 2002). In the next Section we will explore in detail the implications of this delayed response of the air-sea carbon flux to surface forcing. We illustrate the concepts using a Lagrangian frame of reference,

where one follows a hypothetical water column as it moves around the North Atlantic.

4. A LAGRANGIAN VIEW OF AIR-SEA CARBON DIOXIDE FLUXES

We now consider the carbon cycle in the surface mixed-layer, and its response to surface solubility and biological forcing in a Lagrangian frame, following a moving water column. From this point of view, the development of properties of the water parcel can be described without explicit account for transport. (In contrast, in the more usual Eulerian framework, temporal changes are evaluated at a fixed point in space and the advective transfer of properties must be explicitly accounted for). This Lagrangian view is somewhat idealized; we ignore the effects of a vertical shear in the horizontal velocity. Here we will consider idealized trajectories of water columns starting in the tropics, following the Gulf Stream system and then circuiting around the subtropical gyre or passing into the subpolar gyre.

We schematically depict a water column moving within an ocean basin in Fig. 6, illustrating how its change in temperature, T, and nutrient, N, properties affect the air-sea flux of carbon dioxide (see caption). How does the air-sea flux of CO_2 relate to Lagrangian changes in temperature, mixed-layer thickness and nutrient concentration? Significant surface temperature changes can be induced by air-sea heat exchange on timescales as short as a few weeks. Biological drawdown may occur on even shorter timescales. In contrast, the subsequent equilibration of mixed-layer carbon with the overlying atmosphere is relatively slow, occurring on a timescale on the order of a year (Broecker and Peng, 1974). This mismatch in forcing and response timescales means that changes in surface carbon concentration occur downstream of surface temperature and nutrient changes.

4.1 A LAGRANGIAN DESCRIPTION OF THE EVOLUTION OF SURFACE DISSOLVED INORGANIC CARBON

Here we outline an idealized description of the upper ocean carbon cycle which clearly reflects the temporal and spatial separation of forcing and response. We then go on to illustrate this separation in examples using a numerical model. Related Lagrangian approaches to the carbon system have previously been applied by Xu (1990), Follows *et al.* (1996), Brostrom (2000) and Andersson and Olsen (2002).

The Lagrangian change in the surface dissolved inorganic carbon concentration, C, is controlled by the air-sea CO_2 flux, $\mathcal{F}$, the entrainment of carbon,

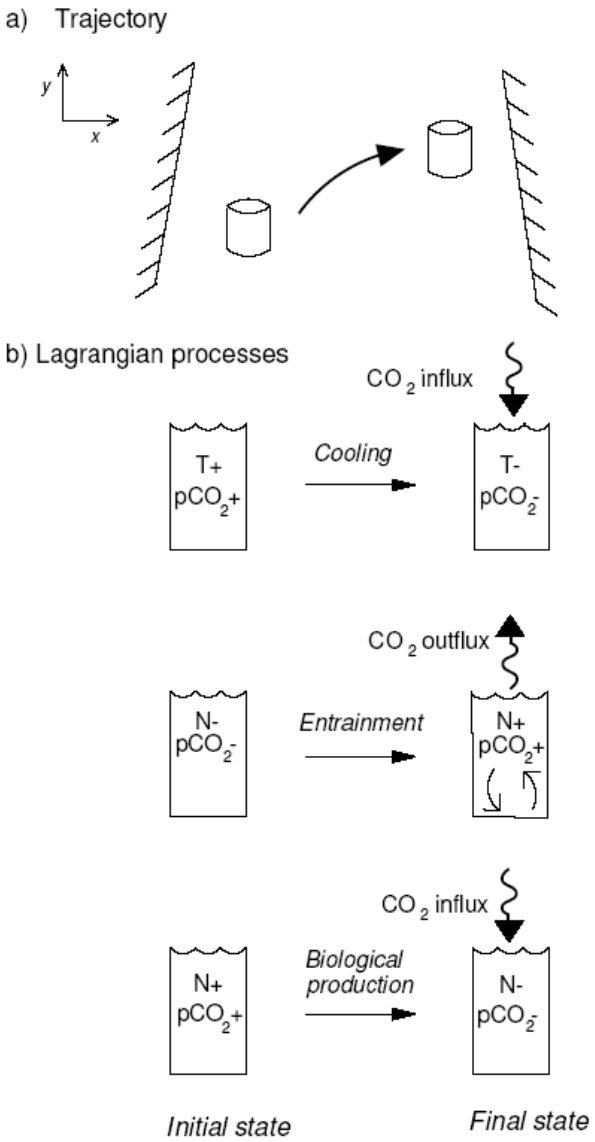

Figure 6. Schematic depiction of a water column moving within an ocean basin and how changes in its properties influence the air-sea flux of carbon dioxide. Cooling and a reduction of surface T increases the solubility and drives an influx of CO_2. However, cooling the surface may also lead to a thickening of the mixed layer and a vertical supply of thermocline waters, nutrient and carbon rich, due to entrainment. Entrained DIC will drive outgassing (or reduce uptake). The presence of nutrients may lead to biological production and reduction of surface DIC, driving an influx of CO_2.

E_C, and the net biological source-sink term, S_C:

$$\begin{array}{ccccccc} \dfrac{DC}{Dt} & = & \dfrac{\mathcal{F}}{h} & + & E_C & + & S_C. \\ storage & & air-sea & & entrain & & biology \end{array} \tag{2}$$

Here the Lagrangian derivative, $D/Dt = \partial/\partial t + \mathbf{u}.\nabla$, denotes the rate of change following the movement of a water column, where $\mathbf{u}$ represents the horizontal velocity vector. $\mathcal{F}$ is the air-sea flux of CO_2 given by (1) and is defined to be positive when the flux is directed into the ocean. h is the thickness of the surface ocean mixed layer. The supply of carbon into the mixed layer through entrainment and upwelling from the thermocline is represented by E_C where $E_C > 0$ for an input of carbon-rich, thermocline waters. The term S_C represents the net supply of carbon due to biological processes. $S_C < 0$ indicates the dominance of consumption of inorganic carbon, and export of the organic matter to the deep ocean, over local remineralization.

4.2 THE EVOLUTION OF SURFACE NUTRIENTS

The governing equation for a nutrient, here phosphorus, in the mixed layer is analogous to that of carbon (2), but the air-sea exchange of nutrients is generally a negligible term (for phosphorus; not necessarily so for nitrogen or iron).

$$\begin{array}{ccccc} \dfrac{DN}{Dt} & = & E_N & + & S_N. \\ storage & & entrain & & biology \end{array} \tag{3}$$

Here, E_N represents the supply of inorganic nutrients through entrainment and upwelling, and S_N the influence of biological processes. The carbon and nutrient relations, (2) and (3), can be combined after the following assumptions: Biological transformations of carbon and nutrients are assumed to occur with fixed stoichiometry; the Redfield ratio, $\mathcal{R}$ (see, for example, Anderson and Totterdell, 2003, this volume). Hence

$$S_C = \mathcal{R} S_N. \tag{4}$$

We relate the entrainment of C and N by

$$E_C = \mathcal{R}_{th} E_N, \tag{5}$$

where $\mathcal{R}_{th}$ is the ratio of the vertical contrast in C and N between the mixed layer and thermocline:

$$\mathcal{R}_{th} = \frac{C_m - C_{th}}{N_m - N_{th}},$$

where subscripts m and th refer to mixed layer and thermocline values.

Thus, the evolution of surface carbon (2) can be re-expressed in terms of nutrient changes by combining it with (3), (4) and (5), and rearranging to give

$$\underset{storage}{\frac{DC}{Dt}} = \underset{air-sea}{\frac{\mathcal{F}}{h}} + \underset{biology}{\mathcal{R}\left(\frac{DN}{Dt} - E_N\right)} + \underset{entrain}{\mathcal{R}_{th}E_N}. \tag{6}$$

Hence, the carbon evolution is now defined in terms of the air-sea flux, the input of carbon from entrainment, and the biological cycling defined in terms of Lagrangian changes in nutrient concentration and entrainment.

Consider an artificial limit where the vertical gradients of carbon and nutrients in the thermocline are set entirely by Redfieldian biological processes, $\mathcal{R}_{th} = \mathcal{R}$. In this case, entrainment has no net effect, since upwelled "biogenic carbon" is simply utilized again as nutrients are consumed (Lewis, 1992). Biological processes can then be described solely in terms of DN/Dt and an increase in surface N implies an accompanying increase in surface C driving an outgassing of CO_2. However, in practice, the vertical gradients of carbon and nutrients are not always in a Redfield ratio due to the air-sea exchange of CO_2 leading to differences in the ratio of the surface C and N, which are then subducted into the interior.

4.3 A LAGRANGIAN DESCRIPTION FOR THE EVOLUTION OF A CARBON ANOMALY

It is convenient to express these relationships in terms of C', the disequilibrium of surface ocean and atmospheric carbon

$$C' = C - C^{eq}, \tag{7}$$

where C is the dissolved inorganic carbon concentration and C^{eq} the local equilibrium value; the concentration at which the water parcel would be in balance with the pCO_2 in the overlying atmosphere at the current temperature, T, salinity, S, and alkalinity. It can be shown that the air-sea flux of carbon may be approximated as a function of C' (see Appendix A):

$$\frac{\mathcal{F}}{h} = -\frac{C'}{\tau}, \tag{8}$$

where τ represents an equilibration timescale for carbon in the mixed layer which is of the order of 1 year; $\tau^{-1} = K_g\alpha_o\beta/h$; here, β is the buffer factor and $\alpha_o = [CO_2]/C$ at local equilibrium (Appendix A).

Substituting for C and $\mathcal{F}/h$ from (7) and (8) in (6) we rewrite the governing equation for surface carbon in terms of the disequilibrium:

$$\frac{DC'}{Dt} = -\frac{C'}{\tau} - \frac{DC^{eq}}{Dt} + \mathcal{R}\frac{DN}{Dt} + (\mathcal{R}_{th} - \mathcal{R})E_N. \tag{9}$$

Following a water column, (9) describes the development of the disequilibrium (i.e. difference from equilibrium with overlying atmosphere) of dissolved inorganic carbon in the surface waters. The first term on the right represents the decay of the disequilibrium due to air-sea gas transfer. The second term represents the forcing due to changes in the local equilibrium carbon concentration; a function of temperature, salinity and alkalinity which is largely determined by physical influences, though the production of calcium carbonate by organisms does affect alkalinity (for simplicity, we do not address this issue further here). The second term might, for example, reflect the increase in equilibrium carbon concentration as a water parcel cools during a poleward transit. The third and fourth terms together represent the combined effects of entrainment and biological cycling as in (6).

We can rearrange (9) in terms of the carbon anomaly to give

$$\frac{DC'}{Dt} + \frac{C'}{\tau} = \mathbf{F}(\mathbf{t}), \tag{10}$$

where $\mathbf{F}(\mathbf{t})$ represents the sum of the forcing terms following the parcel:
$\mathbf{F}(\mathbf{t}) \equiv -\frac{DC^{eq}}{Dt} + \mathcal{R}\frac{DN}{Dt} + (\mathcal{R}_{th} - \mathcal{R})E_N$.
Since the air-sea flux, $\mathcal{F} = -K_0 K_g p' = -hC'/\tau$, the relationship in (9) can also be expressed in terms of the air-sea partial pressure difference, p';

$$\frac{D(K_g K_0 p')}{Dt} + \frac{K_0 K_g p'}{h} = \mathbf{F}(\mathbf{t})\ . \tag{11}$$

Though the air-sea partial pressure difference, p', is perhaps a more tangible quantity than the disequilibrium expressed as a DIC anomaly, C', the prognostic equation for p', (11), is not so clean since the solubility coefficient, also a function of temperature and salinity, K_0 now appears explicitly inside the derivative.

4.4 LAGGED RESPONSE OF THE CARBON SYSTEM TO EXTERNAL FORCING

In this framework, it is easy to illustrate the lagged response of the carbon system to external physical or biological forcing if we study the case where the forcing terms, $\mathbf{F}$, and the equilibration timescale, τ, are constant over a period of time, t. Assuming that the water parcel starts out at time $t = 0$ with initial carbon anomaly, $C'(0)$, and that the forcing, $\mathbf{F}$, is constant in time, we can

solve (10) for the temporal development of the disequilibrium:

$$C'(t) = C'(0)e^{-t/\tau} + \tau\mathbf{F}\left(1 - e^{-t/\tau}\right). \tag{12}$$

The carbon anomaly, $C'(t)$, depends on (i) the initial disequilibrium with the atmosphere, $C'(0)$, which decreases with time as the air-sea flux erodes the anomaly, and (ii) the additional disequilibrium caused by the physical or biological forcing over time t, inducing a further air-sea flux. Notice that the timescale for the decay of the initial anomaly, and the subsequently induced anomalies, is τ which is typically on the order of a year or more and comparable with the residence time of a water parcel in the surface waters with respect to subduction into the thermocline.

Again, since $\mathcal{F} = -hC'/\tau$, the expression for the change in C' can be expressed in terms of the air-sea flux, $\mathcal{F}$,

$$\mathcal{F}(t) = \mathcal{F}(0)e^{-t/\tau} - h\mathbf{F}\left(1 - e^{-t/\tau}\right). \tag{13}$$

The air-sea flux at a time t is likewise controlled by (i) the initial air-sea flux at time $t = 0$, in response to the initial disequilibrium, which decays as the anomaly is eroded, and (ii) the additional flux created in response to a change in the equilibrium carbon concentration due to external forcing over the time t.

In summary, we have presented an idealized description of the surface ocean carbon system in the Lagrangian frame which brings out clearly the lagged response of the surface disequilibrium and air-sea flux to physical and biological forcing. In the following section we illustrate the consequences of this lagged response, in a qualitative sense, using a numerical model.

5. AN UPPER OCEAN WATER COLUMN MODEL.

We now illustrate this point, and the relationships between the air-sea flux and forcing using a more detailed one-dimensional model with which we can explore more complex situations; for example, with time varying forcing. The model resolves the vertical structure of a water column moving around the surface ocean. It includes explicit descriptions of the carbonate chemistry system and biological export of nutrients and carbon.

5.1 FORMULATION OF THE ONE-DIMENSIONAL MODEL

The model represents a one-dimensional (depth) column of water which we imagine to be swept around the surface of the North Atlantic. Though the model is more detailed than the simplified mathematical description above it is still highly idealized and assumes that the water column is isolated from the waters surrounding it and that there is no vertical shear in the flow; in other

words the water column remains vertical during its passage around the gyres. We resolve the vertical structure of tracers, including temperature, salinity, dissolved inorganic carbon and nutrients. They are transported within the column by an imposed "diffusive" mixing or convective adjustment. If the water column becomes unstable due to surface cooling, i.e. if the surface density exceeds that at depth, then the water column and its properties are vigorously mixed until a homogeneous vertical density profile is achieved. Conversely, if we warm the surface ocean, the the mixed-layer depth shallows and water is subducted into the thermocline. We solve for the full carbonate chemistry system (see Murray, 2003, this volume) and specify the biological consumption and export of nutrients in the euphotic zone (upper 100m). CO_2 is exchanged with the atmosphere which has a fixed pCO_2 of 280$ppmv$ according to the changes in the carbonate chemistry sytem and an imposed gas transfer coefficient, K_g.

Using this simple, but explicit model, we illustrate the respsonse of the surface carbon system and air-sea flux to imposed changes in physical conditions, consistent with idealized trajectories around the surface North Atlantic ocean. The key point illustrated is the lag in the response of the air-sea flux of carbon, and decay of induced dissolved inorganic carbon anomalies, induced by physical or biological forcing. We have applied a similar approach, in a abiotic framework, in Follows *et al.* (1996) and some relevant detail may be found in that article.

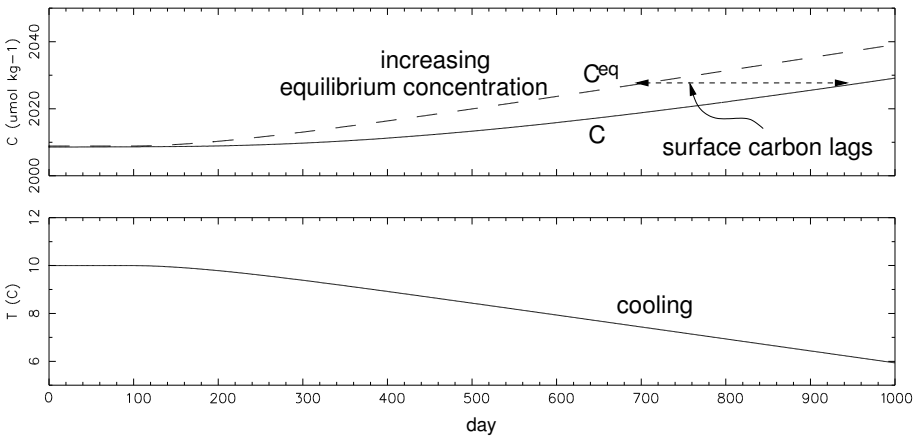

Figure 7. Change in surface properties and air-sea carbon flux following an idealized water column moving through the surface ocean. In this case the mixed layer depth is unchanging (120 m) and the water parcel is initially at equilibrium with the overlying atmosphere for the local temperature and salinity. The panels show: (a) C, solid line, and C^{eq}, dashed line ($mol\ m^{-3}$); (b) mixed-layer temperature (^oC) following the water parcel.

5.2 RESPONSE TO COOLING: THE ABIOTIC LIMIT WITH NO ENTRAINMENT OR UPWELLING

If the water column is cooled C^{eq} increases, creating a negative surface DIC anomaly, C', (and an air-sea difference in pCO_2) inducing a flux of carbon into the ocean. The example in Fig. 7 clearly illustrates the lagged response to a sustained cooling of the mixed layer: C^{eq} increases ahead of C (dashed and full lines respectively in Fig. 7a). The forcing leads the response by about a year in accord with the interpretation of the simplified theory in (12) and (13).

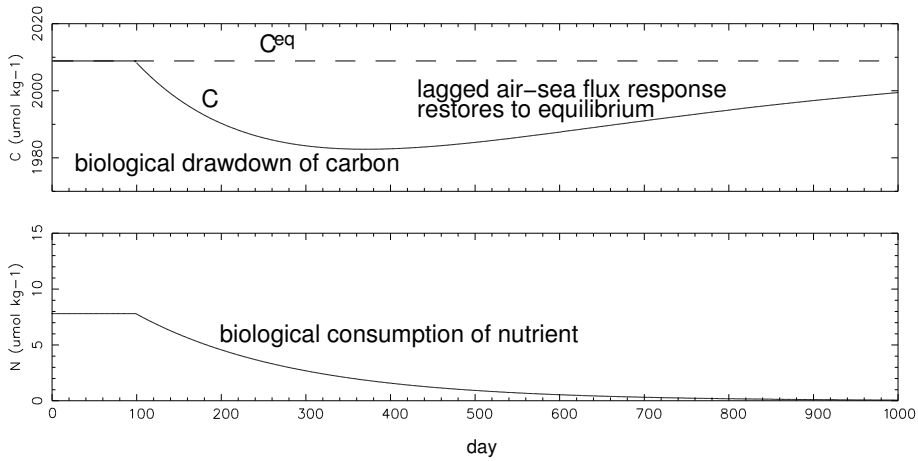

Figure 8. Change in surface properties and air-sea carbon flux following a water column moving through the surface ocean. In this case the mixed layer depth is unchanging (100 m) and the water parcel is initially at equilibrium with the overlying atmosphere for the local temperature and salinity. The panels show: (a) C, solid line, and C^{eq}, dashed line ($mol\ m^{-3}$); (b) nitrate concentration ($mol\ m^{-3}$) following the water parcel.

5.3 RESPONSE TO BIOLOGICAL DRAWDOWN

If surface nutrient, N, decreases through biological consumption and formation of organic matter, then a negative surface C' (i.e. undersaturation) is formed driving an air-sea flux of CO_2 into the ocean. In contrast with the cooling case above, the anomaly is driven by a loss of C from the water column as opposed to change in the equilibrium value, C_{EQ}. We illustrate a simple case from the simplified numerical model in which the mixed-layer temperature and thickness are held constant, but nutrients and carbon and biologically consumed. Since the equilibrium carbon concentration, C^{eq}, is a function only of temperature and salinity here (and alkalinity is fixed), it does not change in response to the nutrient drawdown and there is a subsequent air-sea flux of

carbon compensating for the biological drawdown. However, the air-sea flux occurs with a time lag on the order of a year, consistent with the theory outlined in the previous section.

5.4 WITH THERMAL AND BIOLOGICAL FORCING AND ENTRAINMENT: SUBPOLAR AND SUBTROPICAL PATHWAYS

Now we consider two more realistic, though still idealized, trajectories; the first passing through the Gulf Stream and circuiting into the subpolar gyre, and the second passing through the Gulf Stream and circuiting into the subtropical gyre (Fig. 9). We will examine these pathways in the context of the theory and the numerical model. In order to clearly demonstrate the key gyre-scale interactions we do not resolve the seasonal cycle though this could modify details of the results (Brostrom, 1997). Figures 10 and 11 illustrate the surface ocean carbon cycle processes in these idealized pathways and again we emphasize the impact of the lagged response.

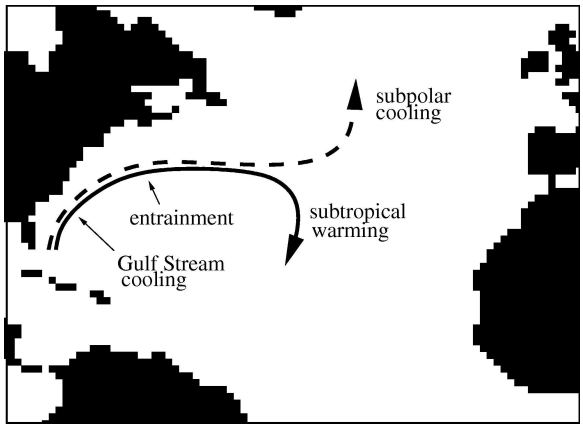

Figure 9. Idealized pathways for surface water parcels in the North Atlantic basin. Both parcels start out moving northwards through the Gulf Stream system where they cool strongly. At the inter-gyre boundary the water columns form deep winter mixed-layers, as a result of the cooling, and move into the interior of the basin. One water column is caught in the anticyclonic flow of the subtropical gyre, returning southwards with a warming and shoaling mixed layer. The other water column is caught in the cyclonic subpolar flow and continues to move polewards with increasing mixed layer thickness and surface cooling.

In the subpolar example, the water column starts its transit close to equilibrium with the overlying atmosphere and the surface depleted of nutrients (Fig. 10). It transits through the Gulf Stream system experiencing cooling, increased solubility, but also thickening of the mixed layer and entrainment of nutrients and carbon to the surface. There is a large air-sea flux of CO_2 directed into

the ocean over the subpolar gyre (reflected in the increased disequilibrium), which is due to downstream cooling increasing C^{eq} and reinforced by the reduction in C due to biological consumption. In this ideal trajectory, the water column continues to cool as it circulates in the subpolar gyre, and so continues to absorb atmospheric CO_2 at a greater rate.

In this particular experiment, the downstream entrainment and subsequent biological export of N enhances drawdown of CO_2; C decreases even though C^{eq} is increasing because $(\mathcal{R}_{th} - \mathcal{R}) > 0$. If, in contrast to the example shown, $(\mathcal{R}_{th} - \mathcal{R}) < 0$, then entrainment of thermocline waters will bring excess carbon, over and above that required to support biological export of the entrained nutrients, and partially compensate for the increased solubility due to cooling, reducing the uptake of CO_2 from the atmosphere. Mahadevan *et al.* (2002) have mapped $\mathcal{R}/\mathcal{R}_{th}$ in the global oceans. Their analysis suggests that regions of both positive and negative $(\mathcal{R}_{th} - \mathcal{R})$ are present in the subpolar North Atlantic implying that entrainment can alter both the sign and magnitude of the air-sea flux of CO_2.

In the subtropical example, the water column follows a similar pathway through the Gulf Stream, but then recirculates and moves into the interior of the subtropical gyre where the surface water is warmed and the mixed layer shoals (Fig. 11). Despite the warming, the surface water remains under-saturated, C is always below C^{eq}. There is an uptake of CO_2 from the atmosphere in the interior of the subtropical gyre due to both the drawdown of nutrients and, significantly, the lagged response to the upstream cooling as illustrated in Fig. 7. The subtropical and subpolar responses differ in the subduction peak associated with the rapid mixed-layer shoaling in the subtropical case (Fig. 11). The shoaling leads to a decrease in the mixed-layer equilibration timescale (Appendix A) and thus downstream decrease in disequilibrium: C approaches C^{eq}.

In summary, as the idealized examples suggest, the surface carbon concentration rarely reaches a local equilibrium with the overlying atmosphere (witnessed by Fig. 1). This disequilibrium is due to the continual forcing induced by the physical and biological processes, changing the equilibrium carbon concentration (by changes in T, S and alkalinity) and changes in nutrient concentrations. Incorporating a seasonal cycle introduces more rapid changes in the equilibrium conditions. The exchange timescale, τ, seasonally varies from a few months over summer to several years in winter due to the thickening of the mixed layer which extends the delay in the response of the carbon flux to large scale changes in forcing. This mismatch in forcing and response timescales leads to changes in surface carbon concentration occurring downstream of surface temperature and nutrient changes.

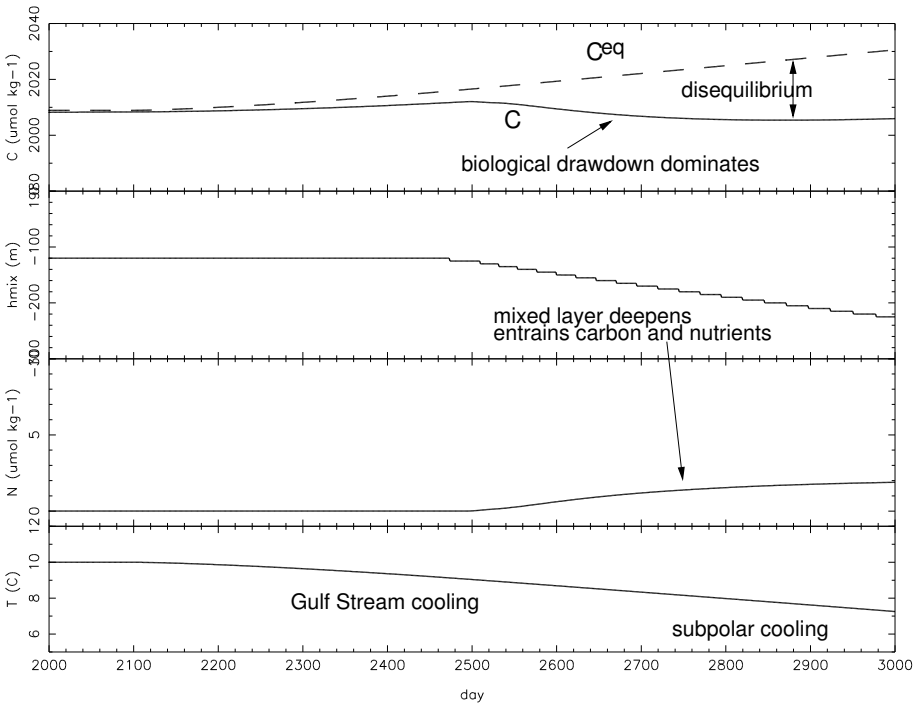

Figure 10. Subpolar example: evolution of surface carbon system following water column on an idealized trajectory through the Gulf Stream system and into the subpolar gyre (dashed line Fig. 9). While cooling increases solubility and promotes an uptake of CO_2 entrainment of nutrients promotes biological drawdown which dominates the trend of C in the subpolar gyre. **(a)** C, solid line, and C^{eq}, dashed line ($mol\ m^{-3}$); **(b)** mixed-layer thickness (m); **(c)** nitrate concentration ($mol\ m^{-3}$); **(d)** mixed-layer temperature (^oC), and **(e)** cumulative flux of carbon into the ocean ($mol\ m^{-2}$), following the water parcel.

6. SUBDUCTION OF CARBON INTO THE THERMOCLINE

The ocean interior acquires its water-mass structure, such as temperature, salinity, and stratification, principally through the ventilation process, where fluid in the surface mixed layer (in contact with the atmosphere) is transferred into the main thermocline and deep ocean. In addition the properties at the point of ventilation also affect the interior carbon, nutrient and dissolved gas distributions.

Ventilation over the open ocean can be separated into deep convection and the subduction processes. Both processes occur preferentially at the end of winter when the mixed layer is at its maximum thickness and density. Deep convection occurs where there is strong surface buoyancy loss and favourable pre-conditioning with a doming up of isopycnals. The surface buoyancy loss in

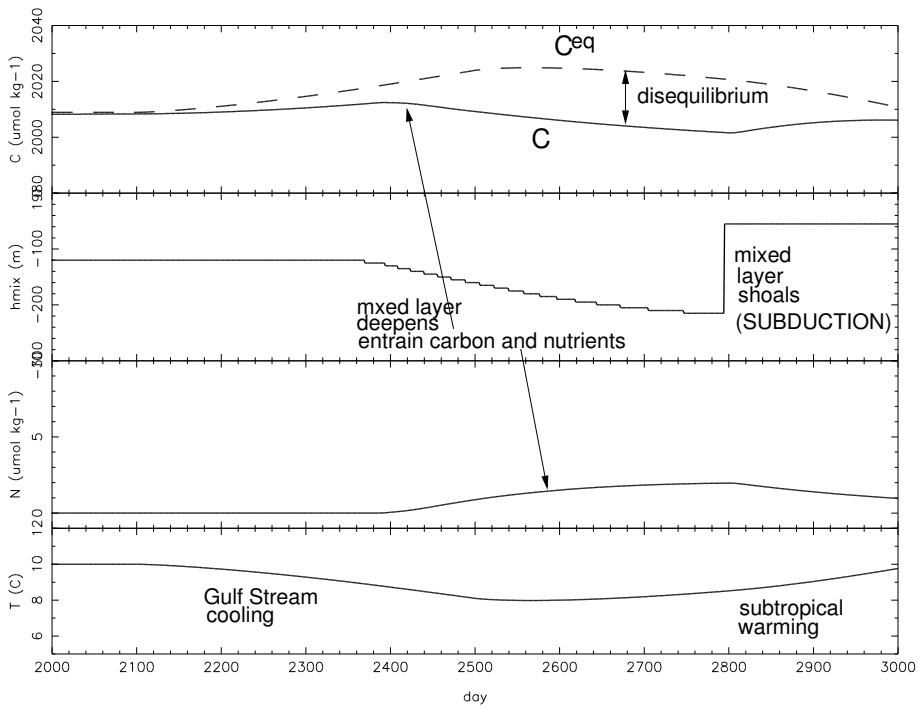

Figure 11. Subtropical example: evolution of surface carbon system following a water column on an idealized trajectory through the Gulf Stream system and into the subtropical gyre (solid line, Fig. 9). Note that the surface waters are undersaturated, and drawing CO_2 from the atmosphere even in the subtropical gyre where the water column is warming. This is, in part, due to the lagged response to cooling upstream in the Gulf Stream system. Panels are as in Fig. 10.

winter erodes the relatively thin, thermocline and lead to striking overturning (see review by Marshall and Schott, 1999). The overturned fluid then spreads from the convective sites through boundary currents if there are topographic barriers or through geostrophic eddies. In the North Atlantic deep convection occurs in very localized regions of the Labrador and Greenland Seas.

Subduction occurs principally over the interior of the subtropical gyres, where fluid is transferred into the main thermocline through a combination of downwelling and a lateral transfer through a shoaling mixed layer (Fig. 12a); see North Atlantic study by Marshall et al. (1993) and review by Williams (2001). Over the North Atlantic, the subduction rate estimated from climatology reveals a high band downstream of the Gulf Stream in the subtropical gyre and lower values elsewhere over the subtropical gyre (Fig. 12b). Conversely, fluid is transferred from the thermocline into the mixed layer over much of

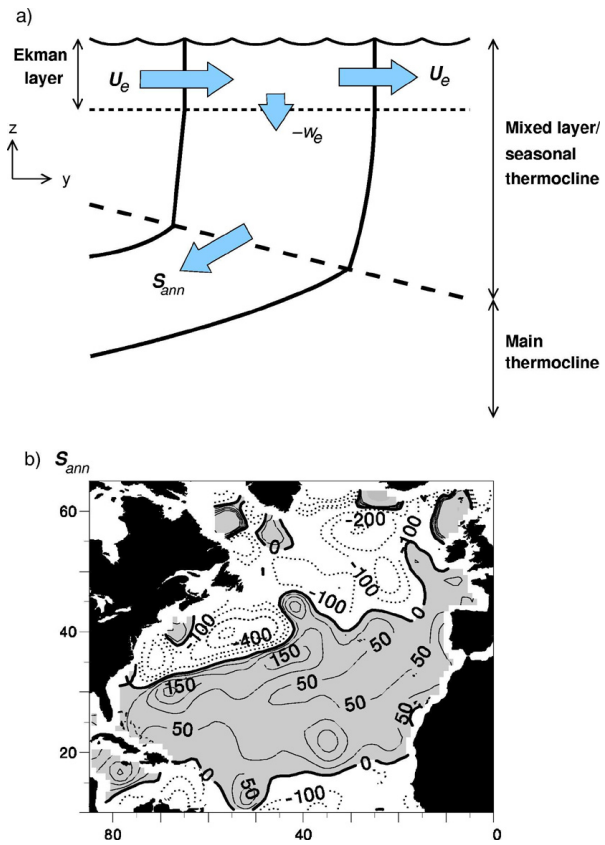

Figure 12. **(a)** Schematic representation of the subduction process where fluid is transferred from the mixed layer into the stratified thermocline. **(b)** subduction rate or volume flux per unit horizontal area into the main thermocline ($m\ y^{-1}$) over the North Atlantic; see Marshall *et al.* (1993) for details.

the subpolar gyre. This gyre-scale contribution to subduction can also be augmented by eddy or frontal-scale contributions (Marshall, 1997).

The ventilation process peaks over certain regions and leads to the formation of 'mode waters', characterized by their weak stratification and extensive volume. For example, the band of enhanced subduction downstream of the Gulf Stream is associated with the formation of 18°C Water, and the continual entrainment and thickening of the mixed layer as fluid moves anti-cyclonically around the subpolar gyre eventually leads to the formation of Labrador Sea Water. These 'mode waters' and their passage around the ocean represent the dominant physical pathway for carbon to be transferred into the ocean interior; see the review on mode waters by Hanawa and Talley (2001) and the nutrient-related study of Sarmiento *et al.* (2003).

6.1 CONSEQUENCES FOR ATMOSPHERIC CO_2

The ventilated thermocline is on the order of a few hundred metres thick throughout the large subtropical gyres of the world's oceans. Consequently, the thermocline represents significant reservoir of carbon which, if changed on a global scale, may have a significant impact on atmospheric pCO_2 (Follows *et al.*, 2002; Ito and Follows, 2003). The carbon properties of the thermocline, with respect to the solubility pump, are set at the point of subduction. The biological pump subsequently modifies these waters as they transit through the interior. The region of maximum subduction rate in the North Atlantic is also a place where the surface waters are strongly undersaturated and absorbing CO_2 following recent vigorous cooling in the Gulf Stream (Fig. 5a, Fig. 12). Also note the undersaturation at the point of subduction in the idealized water column model shown in Figure 11. Hence, subducted waters are undersaturated and the thermocline stores less carbon than if full saturation were achieved before subduction.

For a closed ocean-atmosphere system, thickening the thermocline can lead to an increase in the volume of warm waters, a reduction in the mean solubility of CO_2 in the ocean, and a net transfer of carbon from ocean to atmosphere. Reducing the saturation state of the subducted waters will have the same effect. The saturation state depends upon how long it takes water parcels to be advected through the Western Boundary Current system relative to the air-sea equilibration timescale. The wind-stress forcing on the ocean has a significant influence on both the thickness of the ventilated thermocline and the swiftness of the boundary currents. Theoretical arguments and numerical model experiments (Ito and Follows, 2003) suggest that a factor of two change in wind-stress forcing on the ocean could lead to changes in atmospheric pCO_2 of as much as 30$ppmv$ by modulating the volume and saturation state of the thermocline waters (see Fig. 13).

7. EFFECT OF TIME-VARYING, EDDY CIRCULATIONS

We have discussed processes and interactions on the basin and gyre scales, but there is significant energy in motions on much smaller scales in the ocean; geostrophic eddies on scales of tens to one or two hundred kilometres, and even smaller frontal scales. In principle, such time-varying, finer-scale circulations alter the structure of the upper ocean and thus the exchange of heat and dissolved gases with the atmosphere. With respect to biological productivity, there has been much discussion of the importance of mesoscale eddies (McGillicuddy et al., 1998; Oschlies, 2002), propagation of planetary waves for biological production (Uz et al., 2001; Cipollini et al., 2001), and frontal scale circulations (Mahadevan and Archer, 2000; Levy et al., 2001). Across

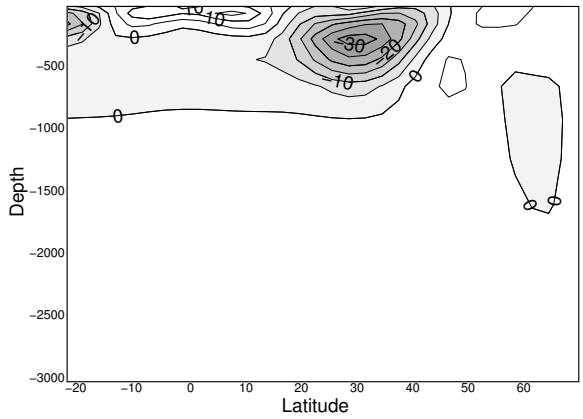

Figure 13. Difference in zonally averaged DIC of two numerical models of the solubility pump in a single ocean basin; one with and one without wind forcing. The basin is about the size of the North Atlantic ocean and is coupled to an atmospheric reservoir of CO_2 through air-sea exchange. Introducing wind-stress forcing has developed thick, warm thermocline in the upper few hundred metres. Due to the swiftness of the Western Boundary Current which feeds the region of subduction, the waters of the thermocline are significantly under-saturated with DIC concentrations as much as $30\mu M$ less than the case without wind forcing. The deep ocean DIC is largely unchanged. In this simplified model a doubling of wind-stress forcing can lead to a greater outgassing of carbon from the ocean and an increase in atmospheric pCO_2 of as much as $30ppmv$.

this range of scales there are deformations of the near-surface isopycnals which may be reversible or irreversible.

The extent to which these time-varying circulations are significant for the air-sea exchange of CO_2 is, as yet, unquantified. However it is clear that their importance for the air-sea exchange of CO_2 partly depends on how persistent these phenomena are relative to the air-sea equilibration timescale, whether there is associated biological activity, and whether there is any modification of the surface mixed-layer.

In the following thought experiments we consider how the air-sea flux might change in response to idealized, eddy-induced changes in surface ocean DIC and N concentrations. In these examples we consider the impact of a persistent eddy or "ring" as it moves through the ocean. (We note that there may be associated perturbations of temperature and alkalinity which are significant for the carbon system but, for simplicity, we will not discuss them further here).

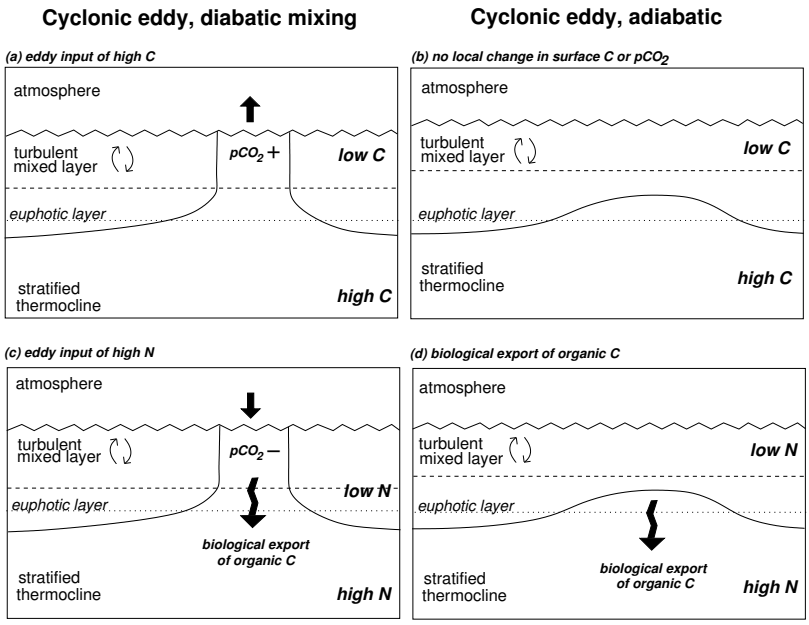

Figure 14. Schematic depiction of the biogeochemical influences of cyclonic eddies in circumstances where either isopycnal surfaces are lifted and mixed into the surface mixed-layer (left panels), or they are not mixed to the surface but are deformed into the sunlit euphotic layer (right panels). The turbulent mixed layer (with its base denoted by a dashed line) overlies a stratified thermocline. Here we examine cases where the euphotic layer (its base denoted by dotted line) is deeper than the mixed-layer. The full line denotes an isoline separating low C and N surface waters from the thermocline, richer in C and N.
In the left panels, a cyclonic eddy has a raised thermocline and nutricline in contact with the surface mixed-layer where convection bring anomalies of C and N to the surface. The enrichment of surface C promotes outgassing (top left) while the entrainment of nutrients leads to enhanced biological drawdown with the opposite effect (bottom left).
The right panels depict a case where the thermocline undulations do not reach the surface mixed-layer. There is no direct carbon anomaly at the surface (top right) but nutrients may be lifted into the euphotic layer (bottom right), promoting production and export of organic matter. In the latter case, even though the carbon profile is changed below the mixed-layer, there is not a local, contemporary expression in surface pCO_2 or air-sea exchange.
In contrast to these cases, anti-cyclonic eddies have a depressed thermocline and nutricline, thus having little effect on the air-sea flux of CO_2 or in biological production.

7.1 IRREVERSIBLY RAISED THERMOCLINE AND INJECTION OF DIC AND N INTO THE MIXED LAYER

Injection of DIC and N into the mixed layer from below might occur within a travelling cyclonic eddy (Fig. 14a). Thermocline waters are raised into, and irreversibly mixed with, the mixed layer, injecting DIC from the cooler ther-

mocline. This promotes outgassing of CO_2 into the atmosphere *if* other mixed layer properties are constant. Equilibration with the atmosphere takes several seasons to a year (see Fig. 7).

A supply of nutrient, N, into the mixed layer by raising the nutricline (Fig. 14b), promotes phytoplankton growth within the euphotic zone and, ultimately, the export of nutrients and carbon to the deep ocean in organic form. The sign of the induced air-sea exchange of carbon depends on whether the $C : N$ ratio of the thermocline waters raised into the mixed layer is greater or lesser than that in the organic matter (Lewis, 1992; Mahadevan *et al.*, 2002). This is illustrated in the biology and entrainment terms in (6) where the net forcing due to entrainment, $E_N(R_{th} - R)$, changes sign depending on these relative $C : N$ ratios.

The counter-example of an anti-cyclonic eddy with a depressed thermocline is unlikely to lead to changes in air-sea flux or enhancement of biological production since there will be no surface DIC perturbation and the nutricline is pushed downwards, away from the sunlit euphotic zone and the surface mixed layer.

7.2 REVERSIBLE OSCILLATIONS OF THE THERMOCLINE

An undulating thermocline signal, possibly associated with the passage of eddies or planetary waves, need not penetrate into the surface mixed layer. In this case, we regard these thermocline undulations as reversible.

In this case there will be no concurrent, local surface expression of the eddy in DIC or N and no immediate response in surface pCO_2 and gas exchange (Fig. 14c,d). However, there may still be a rectified biological response to such perturbations. During the upwelling phase nutrient rich waters are uplifted into the illuminated, euphotic zone, assuming it extends below the surface mixed-layer. Here photosynthesis can consume N and DIC as long as there is sufficient time for phytoplankton to grow; typically on the order of days (McGillicuddy and Robinson *et al.*, 1997). Thus, the oscillating signal can lead to an enhancement of export of organic carbon to the deep ocean (Fig. 14d). This situation might occur in the tropical oceans, or summer subtropics, where the euphotic zone is deep and mixed-layers are shallow. While these anomalies in DIC created below the mixed layer and in the upper thermocline will not lead to an immediate response in the air-sea flux, there will be a delayed response if the DIC anomaly becomes entrained into the mixed layer in the following winter.

In addition to inducing direct changes in the air-sea flux of carbon there are more subtle and indirect effects of the smaller-scale, time-varying motions (see review by Williams and Follows, 2003). For example, eddies lead to

slantwise exchange of fluid parcels on frontal and eddy scales, increasing the stratification and suppressing convection (Levy et al., 1998; Nurser and Zhang, 2000) and impacting upon surface DIC distribution and air-sea fluxes. Likewise, eddies provide an additional transport (in addition to the time-mean circulation), which can alter the subduction process (Marshall, 1997) and the transport of carbon and nutrients within the thermocline (Lee and Williams, 2000), which is particularly important in the Southern Ocean.

In contrast with the recent focus on the role of vertical meso-scale and submeso-scale motions, Mahadevan *et al.* (2002) suggest that lateral displacements of surface properties by eddies probably play a greater role in modulating surface pCO_2 than the associated vertical excursions.

In summary, it is presently unclear as to the systematic response of the carbon system to the presence of eddies and time-varying circulations. Their importance depends on how persistent the phenomena are relative to the air-sea equilibration timescale, whether there is associated biological activity, and whether there is any modification of the surface mixed-layer. The long term response for the air-sea exchange of CO_2 is also sensitive to the way in which eddies systematically alter the stratification, and vertical and horizontal transports of carbon and nutrients.

8. SEASONAL AND INTERANNUAL VARIATIONS IN THE NORTH ATLANTIC

So far, we have focussed on the large scale structures which control the regional pattern of the annual mean air-sea carbon flux, and the potential of smaller scale motions to influence those patterns. There is a vigorous seasonal cycle in the North Atlantic air-sea carbon flux driven by seasonal sea-surface temperature change and the annual cycle in mixed-layer depth. There is also interannual variability in the air-sea flux of CO_2 driven by changes in the physical environment and biological community.

The variability in the subtropical North Atlantic, has been characterized at the Bermuda Atlantic Time-Series Station (BATS), summarized and discussed by Bates (2000). Seasonal and interannual variability in the CO_2 flux at that site is strongly related to temperature changes and the variability in winter-time convective mixing. Such physical variations can be related to the North Atlantic Oscillation (NAO) index (Hurrell *et al.*, 2003); a measure of the sea level pressure difference between Iceland and Portugal. The NAO index captures a significant fraction of the regional variability in the atmosphere and surface ocean physical properties. A characteristic of the variability often associated with the NAO is the change in winter-time convective mixing. During the high index phase of the NAO, winter mixed layers in the subpolar North Atlantic are anomalously deep, and those in the subtropics anomalously shal-

low (Dickson *et al.*, 1996). The opposite is true during low NAO index winters. The variability in winter mixing can have a direct impact on regional productivity, nutrient and gas fluxes (Bates, 2000; Williams *et al., 2000*; McKinley *et al.*, 2003). Interannual variations in the meteorological forcing can also lead to changes in the rate of subduction and the ventilation of mode waters which can impact on the longer term role of the carbon reservoir in the North Atlantic subtropical thermocline (Bates *et al.*, 2003).

An outstanding question is the role of the North Atlantic as a modulator of the oceanic uptake of fossil fuel CO_2 on interannual timescales. The observations at Bermuda show local variations in the annual flux which, if extrapolated over the whole basin, or whole subtropical gyre, suggest a significant role for the Atlantic in the global variability (Gruber *et al.*, 2002). Atmospheric inverse models concur with this extrapolation. In contrast, experiments with global ocean circulation and biogeochemistry models, which do capture the amplitude of local variability at BATS, do not find significant basin integral variations in the annual air-sea flux (McKinley *et al.*, 2003). Hence, the variability at BATS might in practice not reflect changes over the whole basin, since there can be cancellation from opposing changes in different parts of the gyre.

9. SUMMARY

The air-sea flux of carbon is driven by the disequilibrium between the partial pressure of CO_2 in the surface ocean and atmosphere. This disequilibrium is maintained by a combination of the physical, chemical and biological processes within the ocean.

The extent to which physical or biological processes keep the surface ocean from equilibration, and drive air-sea fluxes of CO_2, depends upon the relative timescale of each process. The air-sea equilibration timescale for CO_2 is relatively long, on the order of one year, and this has significant consequences:
(i) The location of physical or biological forcing and the consequent air-sea flux of CO_2 may be significantly separated in space and time. There is only a simple one to one correspondence between the forcing patterns and the carbon response *if* the air-sea flux response timescale is relatively short compared with the forcing timescale.
(ii) The western boundary currents are swift, the physical forcing (cooling) is strong, and surface water parcels may be subducted shortly after passing through them. Consequently the waters of the main thermocline are probably undersaturated and the ocean's solubility pump is not working at full efficiency. The importance of the thermocline thickness and boundary current speed makes the carbon reservoir of the thermocline sensitive to the wind-stress forcing on the ocean.

(iii) On the basin scale, the disequilibrium between ocean and atmosphere is maintained by the net loss of heat from the North Atlantic ocean and the biological transfer of nutrients from upper waters to depth. The thermal forcing also drives the overturning circulation which facilitates a net oceanic transport of carbon out of the basin to the south.
(iv) The large scale impact of small scale, time-vary structures, such as eddies and fronts, in the ocean is, as yet, unclear. Their affect on the carbon system and air-sea exchange depends on the timescale of the small-scale structures compared with the air-sea equilibration timescale, whether biological production occurs and whether the mixed layer properties are irreversibly modified.
(v) There is significant interannual variability in the surface ocean physical environment which promotes variability of biological productivity and air-sea fluxes. The global significance of North Atlantic variability is yet to be fully quantified.

ACKNOWLEDGMENTS

MJF is grateful for support from NSF grant OCE-0136609. RGW is grateful for support from the UK NERC AMT Consortium Programme NER/O/S/2001. We thank Alison McLaren for discussions and assistance in developing the Lagrangian theory. We thank Amala Mahadevan for an insightful and helpful review

APPENDIX: DEFINING THE TIMESCALE FOR CARBON EQUILIBRATION BETWEEN SURFACE OCEAN AND ATMOSPHERE

In the limit of no entrainment, upwelling or biological processes, the carbon evolution following a water column is controlled by the air-sea exchange:

$$\frac{DC}{Dt} = \frac{\mathcal{F}}{h} = \frac{K_0 K_g}{h}(pCO_2^{at} - pCO_2), \tag{A1}$$

where pCO_2^{atmos} and pCO_2 are the partial pressures of CO_2 in the atmosphere and oceanic mixed layer, K_0 is the solubility of CO_2, K_g is the gas transfer coefficient. The air-sea flux, $\mathcal{F}$, in (A1) may be written in terms of $C' = C - C^{eq}$, the mismatch in total inorganic carbon concentration and its equilibrium with the partial pressure in the atmosphere, pCO_2^{at} at local T and S. Using the buffer factor, β, defined

$$\beta \equiv \frac{pCO_2'/pCO_2^{at}}{C'/C^{eq}}, \tag{A2}$$

and the flux is expressed

$$\mathcal{F} = K_0 K_g \beta \frac{pCO_2^{at}}{C^{eq}}(C^{eq} - C), \tag{A3}$$

The ionization fraction (Stumm and Morgan, 1996) at equilibrium for local conditions, α_0, may be defined

$$\alpha_0 = \frac{K_0\, pCO_2^{at}}{C^{eq}} = \frac{[CO_2]^{eq}}{C^{eq}}. \tag{A4}$$

Substituting from (A4) into (A1) and (A3) relates the carbon evolution to the air-sea forcing expressed in terms of a mismatch between the surface carbon and equilibrium carbon, C^{eq}:

$$\frac{DC}{Dt} = \frac{\mathcal{F}}{h} = \frac{1}{\tau}(C^{eq} - C), \tag{A5}$$

where the exchange timescale for carbon is defined by $\tau^{-1} = K_g \alpha_0 \beta / h$.

Typically for seawater, $\alpha_0 \sim 0.005$ and $\beta \sim 10$ and, if $K_g \sim 10^-4\ m\ s^{-1}$ and $h \sim 100m$, then the timescale τ is estimated to be about 1 $year$.

REFERENCES

Anderson, T. and I. Totterdell (2003) Modelling the response of the oceans biological pump to climate change. This volume.

Andersson, L.G. and A. Olsen (2002) Air-sea flux of anthropogenic carbon dioxide in the North Atlantic *Geophys. Res. Lett.*, **29(19)**, 10.1029/2002GL014820.

Bates, N.R. (2000) Interannual Variability of Oceanic CO2 and Biogeochemical Properties in the Western North Atlantic Subtropical Gyre *Deep-Sea Research II*, **48**, 1507-1528.

Bates N.R., A. C. Pequignet, R. J. Johnson and N. Gruber (2002) A Variable Sink for Atmospheric CO_2 in Subtropical Mode Water of the North Atlantic Ocean, *Nature*, **420**, 489-493.

Broecker, W. S., Peng, T-H., (1974). Gas exchange rates between air and sea. *Tellus*, 26, 21-35.

Brostrom, G. (1997) Air-sea flux of CO_2 - can we shortcut the annual cycle? A Norwegian Sea case study. *Phys. Chem. Earth*, **21**, 517-522.

Brostrom, G. (2000) The role of annual cycles for the air-sea exchange of CO_2. *Marine Chem.*, **72**, 151-169.

Cipollini, P., D. Cromwell, P.G. Challenor and S. Raffaglio, (2001). Rossby waves detected in global ocean colour data. *Geophys. Res. Lett.*, **28**, 323-326.

Conkright, M.E., R.A. Locarnini, H.E. Garcia, T.D. O'Brien, T.P. Boyer, C. Stephens, J.I. Antonov (2002) *World Ocean Atlas 2001: Objective analyses, Data Statistics and Figures. CD-ROM Documentation.* National Oceanographic Data Center, Silver Spring, Maryland.

Dickson, R., J. Lazier, J. Meinke, P. Rhines and J. Swift (1996) Long term coordinated changes in the convective activity of the North Atlantic. *Prog. Oceanogr.*, **38**, 241-295.

Emerson, S., P. Quay, D. Karl, C. Winn, L. Tupas, and M. Landry (1997) The carbon pump in the Subtropical Pacific Ocean: Implications for the Global Carbon Cycle, *Nature* , **389**, 951-954.

Follows, M.J.,T. Ito and J. Marotzke (2002) The ocean's subtropical gyres and Atmospheric pCO2. *Global Biogeochem. Cycles*, **16**, 1113, doi:10.1029/2001GB001786.

Follows, M.J., Williams, R.G., Marshall, J.C., (1996). The solubility pump of carbon in the subtropical gyre of the North Atlantic. *J. Mar. Res.*, **54**, 605–630.

Gruber, N., (1998). Anthropogenic CO_2 in the Atlantic Ocean. *Glob. Biogeochem. Cycles*, **12**, 165-191.

Gruber, N., N.Bates, and C.D. Keeling (2002) Interannual variability in the North Atlantic Ocean carbon sink, *Science*, **298**, 2374-2378.

Hanawa, K. and L.D. Talley (2001) Mode Waters. In *Ocean Circulation and Climate: Observing and Modelling the Global Ocean*, Eds. G. Siedler, J. Church and J. Gould, 373-387.

Hansell, D.A. and C.A. Carlson (1998) Deep ocean gradients in dissolved organic carbon concentrations. *Nature*, **395**, 263-266.

Holfort, J., K.M. Johnson, B. Schneider, G. Siedler and D.W.R. Wallace, (1998) Meridional transport of dissolved inorganic carbon in the South Atlantic Ocean. *Glob. Biogeochem. Cycles*, **12**, 479-499.

Hurrell, J.W., Y. Kushnir, M. Visbeck, and G. Ottersen (2003) An Overview of the North Atlantic Oscillation. in *The North Atlantic Oscillation: Climate Significance and Environmental Impact* J.W. Hurrell, Y. Kushnir, G. Ottersen, and M. Visbeck, Eds. Geophysical Monograph Series, **134**, pp. 1-35.

Ito, T., and M.J. Follows (2003) Upper ocean control of the solubility pump of CO_2. *J. Marine Res.*, accepted for publication.

Josey, S.A., E.C. Kent and P.K. Taylor, (1998). The Southampton Oceanography Centre (SOC) Ocean-Atmosphere Heat, Momentum and Freshwater Flux Atlas. Southampton Oceanography Centre, Reports 6, 30pp.

Lee, M.-M. and R.G. Williams, (2000). The role of eddies in the isopycnic transfer of nutrients and their impact on biological production. *J. Mar. Res.*, **58**, 895-917.

Lefevre, N, A.J. Watson, A. Olsen, A. Rios, F. Perez, T. Johannessen, R. Bellerby, I. Skjelvan, (2003). A decrease in the sink for atmospheric CO_2 in the North Atlantic, To be submitted to *Geophs. Res. Lett.*

Levy, M., L. Memery and G. Madec, (1998). The onset of a bloom after deep winter convection in the northwest Mediterranean sea: mesoscale process study with a primitive equation model. *J. Mar. Sys.*, **16**, 7-21.

Levy, M., P. Klein and A-M. Treguier, (2001). Impact of sub-mesoscale physics on production and subduction of phytoplankton in an oligotrophic regime. *J. Mar. Res.*, **59**, 535-565.

Lewis, M.R. (1992) Satellite ocean color observations of global biogeochemical cycles. In *Primary Productivity and Biogeochemical Cycles in the Sea*. Ed. P.G. Falkowski and A.D. Woodhead, Plenum Press, New York.

Lundberg, L. and P.M. Haugan (1996) A Nordic Seas - Arctic Ocean Carbon Budget from Volume Flows and Inorganic Carbon Data. *Global Biogeochem. Cycles*, **10**, 493-510.

Mahadevan, A. and D. Archer, (2000). Modelling the impact of fronts and mesoscale circulation on the nutrient supply and biogeochemistry of the upper ocean. *J. Geophys. Res.*, **105**, 1209-1225.

Mahadevan, A., M. Levy, and L. Memery (2002) Mesoscale variability of sea surface pCO_2: What does it respond to? *Global Biogeochem. Cycles*, submitted.

Marshall, D., (1997). Subduction of water masses in an eddying ocean. *J. Mar. Res.*, **55**, 201-222.

Marshall, J.C., A.J.G. Nurser and R.G. Williams, (1993). Inferring the subduction rate and period over the North Atlantic. *J. Phys. Oceanogr.*, **23**, 1315-1329.

Marshall, J. and F. Schott, (1999). Open-ocean convection: observations, theory and models. *Rev. Geophysics*, **37**, 1, 1-64.

McGillicuddy, D.J. and A.R. Robinson, (1997). Eddy-induced nutrient supply and new production in the Sargasso Sea. *Deep-Sea Res. I*, **44**, 1427-1449.

McGillicuddy, D.J., A.R. Robinson, D.A. Siegel, H.W. Jannasch, R. Johnson, T. Dickeys, J. McNeil, A.F. Michaels and A.H. Knap, (1998), New evidence for the impact of mesoscale eddies on biogeochemical cycling in the Sargasso Sea. *Nature*, **394**, 263-266.

McKinley, G.A. (2002) Interannual variability of the air-sea fluxes of carbon and oxygen. Ph.D. thesis. Massachusetts Institute of Technology.

McKinley, G.A., M.J. Follows and J.C. Marshall (2003) Mechanisms of interannual variability of the air-sea flux of CO_2. Submitted to *Global Biogeochem. Cycles*.

Murray, J. (2003) Ocean carbonate chemistry. This volume.

Nurser, A.J.G. and J.W. Zhang, (2000), Eddy-induced mixed-layer shallowing and mixed-layer/thermocline exchange. *J. Geophys. Res.*, **105**, 21851-21868.

Orr, J. (2002) Global Ocean Storage of Anthropogenic CO_2: Final Report. EC Environment and Climate Program.

Oschlies, A., (2002) Can eddies make ocean deserts bloom? *Global Biogeochem. Cycles*, **16**, 1106, doi:10.1029/2001GB001830.

Sabine, C.L., R.M. Key, K. Johnson, F.J. Millero, J. Sarmiento, D. Wallace and C. Winn (1999) Anthropogenic CO2 inventory of the Indian Ocean, *Global Biogeochem. Cycles*, **13**, 179-198.

Sarmiento, J.L., Murnane, R., Le Quere, C., (1995). Air-sea CO_2 transfer and the carbon budget of the North Atlantic. *Phil. Trans. Roy. Soc. Lond.*, **B348**, 211–219.

Sarmiento, J.L., N. Gruber, M.A. Brzezinski, and J.P. Dunne (2003) High latitude controls of the global nutricline and low latitude biological productivity. Nature, in press.

Sathyendranath, S., R.S.A. Longhurst, C.M. Caverhill, and T. Platt, (1995). Regionally and seasonally differentiated primary production in the North Atlantic. *Deep-Sea Res. I.*, **42**, 1773-1802.

Schmitz, W.J. and M.S. McCartney, (1993). On the North Atlantic circulation. *Rev. Geophysics.*, **31**, 29-49.

Stumm, W. and J. J. Morgan (1996) *Aquatic Chemistry.* Third Edition. John Wiley and Sons., N.Y., 1022pp.

Takahashi, T., Olafsson, J., Goddard, J.G., Chipman, D.W., Sutherland, S.C., 1993. Seasonal variation of CO_2 and nutrients in the high-latitude surface oceans: a comparative study. *Global Biogeochemical Cycles*, **7**, 843-878.

Takahashi, T., Wanninkhof, R.H., Feely, R.A., Weiss, R.F., Chipman, D.W., Bates, N., Olafsson, J., Sabine, C., Sutherland, S.C., (1999). Net sea-air CO_2 flux over the global ocean: An improved estimate based on the sea-air pCO_2 difference. *Proceedings of the 2nd International Symposium CO_2 in the Oceans*, Ed. Y. Nojiri, Center for Global Environmental Research, CGER-IO37-'99, Tsukuba, Japan, 9-15.

Uz, B.M, J.A. Yoder and V. Osychny, (2001). Pumping of nutrients to ocean surface waters by the action of propagating planetary waves, *Nature*, **409**, 597-600.

Volk T., and M.I. Hoffert (1985) Ocean carbon pumps: Analysis of relative strengths and efficiencies in ocean-driven atmospheric CO2 changes. *Geophys. Monogr.*, **32**, 99-110.

Wallace, D.W.R., (2001). Storage and transport of excess CO_2 in the oceans: the JGOFS/WOCE Global CO_2 survey. In *Ocean Circulation and Climate: Observing and Modelling the Global Ocean*, Eds. G. Siedler, J. Church and J. Gould, 489-521.

Wanninkhof, R. (1992) Relationship between wind speed and gas exchange over the ocean. *Journal of Geophysical Research*, **97**, 7373-7382.

Watson, A.J., P.D. Nightingale and D.J. Cooper, (1995) Modelling atmosphere-ocean CO_2 transfer. *Phil. Trans. Roy. Soc. Lond.*, **B348**, 125-132.

Williams, R.G., (2001). Ocean Subduction. In *Encyclopedia of Ocean Sciences*, Eds. J.H. Steele, K.K. Turekian and S.A. Thorpe, Academic Press, 1982-1992.

Williams R.G. and M.J. Follows, (2003). Physical transport of nutrients and the maintenance of biological production. In *Ocean Biogeochemistry: a JGOFS synthesis*. Ed. M. Fasham, Springer, pp. 19-51.

Williams, R.G., McLaren, A.J., Follows, M.J., (2000). Estimating the convective supply of nitrate and implied variability in export production over the North Atlantic. *Global Biogeochem. Cycles*, **14**, 1299-1313.

Xu, Y.-F. (1990) *A Study of the Biogeochemical Cycle of CO_2 in the Ocean Using a Parcel Model.* Ph.D. thesis. 160 pp. University of East Anglia, Norwich, U.K.

..